

This discussion paper is/has been under review for the journal Atmospheric Chemistry and Physics (ACP). Please refer to the corresponding final paper in ACP if available.

# Metal complexation inhibits the effect of oxalic acid in aerosols as cloud condensation nuclei (CCN)

T. Furukawa and Y. Takahashi

Department of Earth and Planetary Systems Science, Graduate School of Science, Hiroshima University, Higashi-Hiroshima, Hiroshima 739-8526, Japan

Received: 20 October 2010 – Accepted: 27 October 2010 – Published: 9 November 2010

Correspondence to: Y. Takahashi (ytakaha@hiroshima-u.ac.jp)

Published by Copernicus Publications on behalf of the European Geosciences Union.

27099

## Abstract

Atmospheric aerosols have both a direct and an indirect cooling effect that influences the radiative balance at the Earth's surface. It has been estimated that the degree of cooling is large enough to cancel the warming effect of carbon dioxide. Among the cooling factors, secondary organic aerosols (SOA) play a key role in the solar radiation balance in the troposphere as SOA can act as cloud condensation nuclei (CCN) and extend the lifespan of clouds because of their high hygroscopic and water soluble nature. Oxalic acid is one of the major components of SOA, and is produced via several formation pathways in the atmosphere. However, it is not certain whether oxalic acid exists as free oxalic acid or as metal oxalate complexes in aerosols, although there is a marked difference in their solubility in water and their hygroscopicity. We employed X-ray absorption fine structure spectroscopy to characterize the calcium (Ca) and zinc (Zn) in aerosols collected at Tsukuba in Japan with fractionation based on particle size using an impactor aerosol sampler. It was shown that 10–60% and 20–100% of the total Ca and Zn in the finer particles ( $<2.1 \mu\text{m}$ ) were present as Ca and Zn oxalate complexes, respectively. Oxalic acid can act as CCN because of its hygroscopic properties, while metal complexes are not hygroscopic, and so cannot be CCN. Based on the concentration of noncomplexed and metal-complexed oxalate species, we found that most of the oxalic acid is present as metal oxalate complexes in the aerosols, suggesting that oxalic acid does not act as CCN in the atmosphere. Similar results are expected for other dicarboxylic acids, such as malonic and succinic acids. Thus, it is possible that the cooling effect of organic aerosols assumed in various climate modeling studies is overestimated because of the lack of information on metal oxalate complexes in aerosols.

27100

## 1 Introduction

Some anthropogenic aerosols, such as organic aerosols and sulfate aerosols, have a direct cooling effect by scattering solar radiation, and an indirect cooling effect by acting as cloud condensation nuclei (CCN) because of their hygroscopic properties (Novakov and Penner, 1993; Claeys et al., 2004; Kanakidou et al., 2005; IPCC, 2007; Hallquist et al., 2009). The global average contribution of the indirect cooling effect (i.e., the cloud albedo effect) is estimated to be  $-0.3$  to  $-1.8 \text{ W/m}^2$  (Charlson et al., 1992; IPCC, 2007). In the report of the Intergovernmental Panel on Climate Change (IPCC), the sum of the direct and indirect cooling effect of aerosols is almost equivalent to the warming effect of carbon dioxide (IPCC, 2007). However, a large uncertainty exists because of the indirect effect discussed in the IPCC report (2007), which must be evaluated more precisely for a better understanding of the Earth's climate. Thus, a number of studies have been performed on sulfate aerosols and on organic aerosols because of their complex nature in terms of composition and chemical transformation in the atmosphere, and also because of their importance in the global CCN budget (Novakov and Penner, 1993; Claeys et al., 2004; Kanakidou et al., 2005; IPCC, 2007; Hallquist et al., 2009). Among the various organic aerosols studied, water-soluble organic compounds (WSOCs) in aerosols influence the surface environment as they act as CCN because of their hygroscopic properties, and dicarboxylic acids have been identified as a major constituent of organic CCN (Kawamura and Ikushima, 1993; Kawamura and Sakaguchi, 1999; Yao et al., 2002). Moreover, WSOCs increase the cloud albedo effect (i.e., cloud lifetime effect) by extending the lifetime of a cloud depending on their hygroscopic properties (Graham et al., 2004; Lohmann and Leck, 2005; IPCC, 2007). Oxalic acid is a major component of dicarboxylic acids or secondary organic aerosols, and is thought to act as CCN. In this study, we focused on oxalic acid as a representative component of low molecular weight dicarboxylic acids in the atmosphere, and our results can be extended to other dicarboxylic acids, such as malonic and succinic acids.

27101

Oxalic acid can form metal oxalate complexes in aerosols by reacting with metal ions because: (i) aerosols contain various metal ions originating from sea salts, desert dusts, continental soils, and anthropogenic sources; (ii) oxalic acid is formed in the aqueous phase at aerosol surfaces in the atmosphere, which provides a reaction field for metal complexation; and (iii) polyvalent metal ions can form stable complexes with oxalate ions (Warneck, 2003; Graham et al., 2004; Lim et al., 2005; Carlton et al., 2007). However, metal oxalate complexes are not detected using conventional methods, such as gas chromatography and ion chromatography (IC). In the latter analysis, a large volume of water sufficient to dissolve metal oxalate complexes in aerosols is usually employed during the water extraction procedure. In this case, metal oxalate complexes can be readily dissolved, despite the low solubility of some metal oxalate complexes (for more details, see Sect. 3.5), and it is difficult to distinguish between noncomplexed and metal-complexed oxalate species in aerosols. Hence, only a few studies have suggested that WSOCs can react with metal ions and mineral aerosols (Mochida et al., 2003; Sullivan et al., 2007). However, these studies employed indirect methods that cannot show any direct evidence of the formation of metal oxalate complexes in aerosols.

In this study, we applied X-ray absorption fine structure (XAFS) spectroscopy to show the presence of metal oxalate complexes in aerosols, coupled with IC and inductively coupled plasma atomic emission spectrometry (ICP-AES) analyses to determine the ratio of metal oxalate and noncomplexed oxalate species. XAFS data consists of X-ray absorption near edge structure (XANES) and extended X-ray absorption fine structure (EXAFS), which enables us to determine chemical species of each element in aerosols directly (e.g., Takahashi et al., 2006; Higashi and Takahashi, 2009). In the XAFS analysis, size-fractionated aerosol samples were collected during 2002 in the winter (from January to February) and summer (from July to August) in Tsukuba, Japan. Based on our results, it was possible to obtain the ratio of metal-complexed and noncomplexed oxalate species in the aerosols. The ratio determined in this study, coupled with the difference in their hygroscopic properties, can contribute to the precise evaluation of

27102

the role of oxalic acid, or dicarboxylic acids, as CCN.

## 2 Materials and methods

### 2.1 Aerosol samples and characterization

The aerosol samples examined in this study were collected in Tsukuba (a city approximately 60 km northeast of Tokyo: 36.06° N, 140.14° E) in Japan during the winter (21 January to 12 February) and summer (28 July to 13 August) of 2002 (Kanai et al., 2003) as a part of the Japan–China joint “Asian Dust Experiment on Climate Impact” project (Mikami et al., 2006). In this study, size-fractionated aerosol samples were collected using a low-volume Andersen-type air sampler (AN-200, Shibata, Tokyo). The flow rate of the sampler was stabilized at 28.3 L min<sup>-1</sup> to achieve the ideal size separation of the aerosols. The sampler had eight stages and a back-up filter. The particle diameter was classified by the aerodynamic diameter as follows: >11.0 μm (sampling Stage 0), 11.0–7.0 μm (Stage 1), 7.0–4.7 μm (Stage 2), 4.7–3.3 μm (Stage 3), 2.1–3.3 μm (Stage 4), 2.1–1.1 μm (Stage 5), 1.1–0.65 μm (Stage 6), 0.65–0.43 μm (Stage 7), and <0.43 μm (back-up filter). The filters used for Stages 0–6 were Advantec PF050 polyflon filters (diameter = 80 mm, Advantec, Tokyo, Japan). A polyflon filter was used because these filters do not contain any major elements nor do they react with any acid gases during sampling. The filters used for Stage 7 and the back-up filters were Tokyo Dylec 2500QAT-UP quartz filters (Tokyo Dylec, Tokyo, Japan). The filters were weighed before and after sampling with a reading precision of 10 μg after stabilizing the weight under constant humidity in a desiccator. A sample mass >1 mg was preferable when measuring the sample weight using a microbalance, and thus, the sampling period depended on the aerosol concentration in the atmosphere. Three-dimensional air mass back trajectories were calculated at three altitudes using the Hybrid Single-Particle Lagrangian-Integrated Trajectory (HYSPLIT4) model (Draxler and Rolph, 2003).

27103

### 2.2 Water soluble components in the aerosol samples

Bulk chemical analysis of the water soluble components (WSCs) in the aerosol was conducted using the procedure used by Kanai et al. (2005). A 1/8 section of the filter was soaked in a Teflon beaker containing 200 μL of ethanol and 5 mL of MQ water. The WSCs were leached by subjecting the solution to an ultrasonic treatment for a period of 30 min. The water soluble fraction was then recovered as a filtrate after filtration through a 0.20 μm hydrophilic polytetrafluoroethylene filter. The solution containing various extracted ions was used to determine the quantity of major anions (Cl<sup>-</sup>, NO<sub>3</sub><sup>-</sup>, SO<sub>4</sub><sup>2-</sup>, and C<sub>2</sub>O<sub>4</sub><sup>2-</sup>) and cations (Na<sup>+</sup>, NH<sub>4</sub><sup>+</sup>, and K<sup>+</sup>). The WSCs were measured using IC (IC7000, Yokogawa, Japan, relative precision = 2%) employing Shodex IC YK-421 and Shima-pack IC-SA1/-SA1(G) columns for the cations and anions, respectively. The eluent composition was a mixed solution containing 24 mM of boric acid, 5 mM of tartaric acid, and 1 mM of 2,6-pyridine dicarboxylic acid for the cations and 14 mM of NaHCO<sub>3</sub> for the anions. The flow rate of the elutant was 1.0 mL min<sup>-1</sup> for both cations and anions. A part of the extraction solution was used to determine the concentration of the water soluble fraction of Zn<sup>2+</sup>, Ca<sup>2+</sup>, and Mg<sup>2+</sup> using ICP-AES (SPS3500).

### 2.3 XAFS measurements

Calcium (Ca) K-edge XANES experiments were performed at Beamline 9A (Takahashi et al., 2006, 2009) at the KEK Photon Factory in Tsukuba, Japan. Beamline 9A has Si(111) double-crystal monochromators. The beam size was smaller than 1 × 0.5 mm<sup>2</sup> at the sample position. The aerosol samples located on each filter appeared as a dark spot (spot size = 0.5–2 mm), and were directly exposed to the incident X-ray beam. The entire beam path of Beamline 9A was filled with He gas to suppress any X-ray absorption and scattering from air. The energy of the Ca K-edge XANES was calibrated by defining the peak maximum of the XANES data of CaCl<sub>2</sub>·2H<sub>2</sub>O at 4038.1 eV. Two modes, the conversion electron yield (CEY) and the fluorescence yield (FL) modes, were employed to record the Ca K-edge XANES spectra. The CEY mode was used to

27104







### 3.3 Ca oxalate in the finer particles

XAFS measurements at the Ca K-edge were carried out to demonstrate the presence of Ca oxalate complexes in the aerosols. From their stability constants, Ca ions are the dominant divalent metal ion in aerosols that can form stable oxalate complexes (Table 1). Figure 5 shows the spectra of aerosol samples and Ca species used to fit the sample spectra. The fractions of Ca species obtained from the fitting are shown in Table 2, and the results of the XANES spectra of various Ca species are shown in Fig. S2. Based on these results, it is suggested that Ca oxalate was observed in the finer particles as 0.43–2.1  $\mu\text{m}$  and 0.65–2.1  $\mu\text{m}$  during the winter and the summer, respectively. The XANES fitting showed that the Ca oxalate fraction among the total Ca concentration was 10–60% (Fig. 5 and Table 2). The peak in the size distribution of the total oxalate occurred in this particle size range, where Ca oxalate is the main Ca species. In this range, the molar concentration of  $\text{Ca}^{2+}$  ions was lower than that of the total oxalate concentration, supporting the presence of Ca oxalate in this particle size.

Gypsum and Ca nitrate were also observed in the same particle size range, and the XANES spectrum of Ca oxalate was similar to that of gypsum and Ca nitrate (Fig. S2). Assuming that gypsum and Ca nitrate were the end members of Ca in the aerosols in the fitting, then the sample spectra could not be fitted, especially around 4047 eV (Fig. S3). On the other hand, the spectra could be fitted perfectly, even around 4047 eV, by assuming that Ca oxalate was an end member (Fig. S3). This result confirms that Ca oxalate is the main Ca species in the finer particles.

In the coarser particles ( $>2.1 \mu\text{m}$ ), the Ca species determined from the fitting were  $\text{CaCO}_3$  (calcite), gypsum, and anhydrite in both periods (Fig. S2 and Table 2). However, the XANES spectra of the finer particles could not be fitted using these three components (Fig. S4). This result also suggested the presence of Ca oxalate in the finer particles. Gypsum and anhydrite can be formed from sea salt particles or from a reaction of calcite and  $\text{SO}_x$  gas at the particle surface in the atmosphere (Buseck and Pósfai, 1999; Takahashi et al., 2009). Calcium nitrate can be formed from the reaction

27109

of calcite and  $\text{NO}_x$  gas (Krueger et al., 2003; Li and Shao, 2009).

Figure 6 shows the hygroscopic properties of oxalic acid and Ca oxalate. The weight of oxalic acid increased markedly at  $\text{RH}=40\%$  because of the absorption of water, whereas Ca oxalate did not absorb water by a factor of 0.01 compared with oxalic acid. These results suggest that oxalic acid can act as CCN because of its high hygroscopic properties, whereas Ca oxalate cannot. Moreover, it is also suggested that the potential of oxalic acid as CCN can be reduced by the formation of Ca and other metal oxalate complexes, if these metal complexes account for a large proportion of the total oxalate in the aerosol.

### 3.4 Zn oxalate in the finer particles

Although the formation of Ca oxalate was suggested in the previous section, it is still necessary to confirm the results using independent data from other metal ions. Among the various divalent cations that can form stable complexes with oxalate (Table 1), Zn K-edge XAFS data was examined to show the formation of Zn oxalate, or other metal oxalate complexes, because: (i) Zn is the second most abundant divalent cation in the aerosol samples, and (ii) the stability constant of Zn oxalate is large (Table 1).

The Zn species in the aerosols at Tsukuba during the winter and summer were measured using Zn K-edge XANES and EXAFS spectra. Various XANES and EXAFS spectra of standard materials for Zn are shown in Fig. S4. The XANES spectra were obtained for particle sizes of these samples (Fig. 7), while EXAFS spectra were obtained only for the finer particle sizes (Fig. 8) where the Zn concentration was high, since high concentration is essential to obtain high quality EXAFS spectra. Based on the fitting of the XANES spectra (Table 3),  $\text{ZnC}_2\text{O}_4 \cdot 2\text{H}_2\text{O}$  (Zn oxalate) in the aerosols was observed in the finer particles that also contained  $\text{ZnSO}_4 \cdot 7\text{H}_2\text{O}$  (Zn sulfate). On the other hand, the Zn species in the coarser particles were  $\text{ZnCl}_2 \cdot 2\text{H}_2\text{O}$  (Zn chloride),  $\text{ZnCO}_3$  (Zn carbonate), and ZnS (Zn sulfide), the details of which, including the sources of these species in the coarser particles, will be described elsewhere. In this study, the variation of Zn species from finer to coarser particle size is important, because the ef-

27110

fect of oxalate formation should be more marked in the finer particle sizes. Zinc oxalate was not needed to fit the spectra of the coarser particles, but was essential to fit the XANES spectra of the finer particles.

Figure 8 and Table 4 show the fitting of the EXAFS data in  $k$  space and the Zn speciation data, respectively. The fitting results of the EXAFS data are more reliable than that of the XANES data, because EXAFS spectra are dependent on the neighboring atoms, interatomic distances, and coordination number, which are sensitive to the Zn speciation. The ratio of Zn oxalate to total Zn species ( $= [\text{Zn oxalate}]/[\text{Zn}]_{\text{total}}$ ) obtained from the XANES and EXAFS fitting were similar (Tables 3 and 4, Fig. S5), which suggests the presence of Zn oxalate, particularly in the finer particle region. Moreover, the  $[\text{Zn oxalate}]/[\text{Zn}]_{\text{total}}$  ratio in each period clearly increased with decreasing particle size (Tables 3 and 4, Fig. S6). This result shows that Zn oxalate was formed in the aqueous phase at the particle surface, which is caused by the increase in  $[\text{surface area}]/[\text{volume}]$  ratio with decreasing particle size. This result corresponds to the scanning transmission X-ray microscopy data, which suggests that the formation of organic aerosols in Asian aerosols occurs at the particle surface (Maria et al., 2004). In addition, the increase in the fraction of Zn oxalate may reflect that the concentration of free oxalate was higher in the finer particles, because the concentrations of  $\text{Ca}^{2+}$  and  $\text{Mg}^{2+}$  ions ( $=$  competitive ions) decreases with decreasing particle size. This means that free oxalate in the finer particles can react with  $\text{Zn}^{2+}$  ions.

The fitting result of the EXAFS data in the particle size range 2.1–3.3  $\mu\text{m}$  in the summer suggests that Zn oxalate was present in this particle range, but not in the same particle range during the winter (Fig. 8b). The peak in total oxalate concentration in the summer was shifted slightly to the coarser particle size (Fig. 3), where the correlation coefficient of Zn and the total oxalate was higher than that of sulfate (Table S2). This result may be related to a shift in the size distribution of oxalate in summer to a larger particle size, the details of which will be described in Sect. 3.6.

27111

### 3.5 Noncomplexed and metal-complexed oxalate species in the aerosols

In this section, the ratio of metal oxalate complexes to total oxalate or noncomplexed oxalate species will be discussed. For this purpose, the concentration of Ca and Zn oxalates were determined by multiplying: (a) the total concentration of Zn and Ca obtained from ICP-AES data, and (b) the oxalate complex fractions of these ions obtained from XAFS data. On the other hand, the concentration of total oxalate (i.e., the sum of noncomplexed and metal complexed oxalate species) was quantified using IC. The total concentration of oxalate, Ca, and Zn could be obtained using this method despite the low solubility of Ca and Zn oxalate complexes in the water extraction procedure, because these complexes were completely dissolved in our experiments, as we added an excess of water in the water-extraction procedure. For example, the total weight of the aerosols (in the 1/8 cut filter) was  $<1$  mg, or the Ca oxalate on the filter was  $<0.025$  mg assuming that the Ca in the sample was 5 wt% and the fraction of Ca oxalate among the total Ca was 50 mol%. Note that the concentration of Ca and the fraction of Ca oxalate assumed in the calculations were larger than the values measured in our samples. On the other hand, the solubility data (Table 1) showed that the amount of Ca oxalate that could be dissolved in 5 mL of the MQ water employed in this study was 0.035 mg, which was much larger than the 0.025 mg. Thus, the Ca oxalate in the aerosols could be completely dissolved in 5 mL water in our experiments. A similar case can be discussed to validate the Zn oxalate data. Thus, we can obtain the concentrations of the total oxalate, Ca, and Zn in the samples using our water extraction procedure.

The  $\{[\text{Zn oxalate}] + [\text{Ca oxalate}]\}/[\text{oxalate}]_{\text{total}}$  ratio, determined as described above, is important to evaluate whether or not oxalate species have a cooling effect. As discussed in the introduction and in Sect. 3.3, noncomplexed oxalic acid in aerosols can act as CCN and have a cloud lifetime effect (Pang et al., 2001; Grahan et al., 2004; Kanakidou et al., 2005; Lohmann and Leck, 2005; IPCC, 2007; Hallquist et al., 2009; Sullivan et al., 2009), whereas Ca and Zn oxalates do not have this potential because

27112







*Acknowledgements.* We are grateful to H. Kamioka, Y. Kanai, S. Yabuki, and A. Ohta for collecting the aerosol samples in the ADEC project. This research was supported by a Grant-in-Aid for Scientific Research in Priority Areas, “Western Pacific Air–Sea Interaction Study (W-PASS)”. This work was performed with the approval of KEK-PF (2007G669 and 2008G683) and SPring-8 (2009B1383 and 2010A1452). This research is a contribution to the Surface Ocean Lower Atmosphere Study (SOLAS).

## References

- Adachi, K. and Tainosho, Y.: Characterization of heavy metal particles embedded in tire dust, *Environ. Int.*, 30, 1009–1017, 2004.
- 10 Buseck, P. R. and Pósfai, M.: Airborne minerals and related aerosol particles: Effects on climate and the environment, *Proc. Natl. Acad. Sci. USA*, 96, 3372–3379, 1999.
- Carltona, A. G., Turpinb, B. J., Altieric, K. E., Seitzingerc, S., Reffd, A., Lime, H. J., and Ervensf, B.: Atmospheric oxalic acid and SOA production from glyoxal: Results of aqueous photooxidation experiments, *Atmos. Environ.*, 41, 7588–7602, 2007.
- 15 Charlson, R. J., Schwartz, S. E., Hales, J. M., Cess, R. D., Coakley, J. A., Hansen Jr., J. E., and Hofmann, D. J.: Climate forcing by anthropogenic aerosols, *Science*, 255, 423–430, 1992.
- Claeys, M., Graham, B., Vas, G., Wang, W., Vermeylen, R., Pashynska, V., Cafmeyer, J., Guyon, P., Andreae, M. O., Artaxo, P., and Maenhaut, W.: Formation of secondary organic aerosols through photooxidation of isoprene, *Science*, 303, 1173–1176, 2004.
- 20 Clegg, N. A. and Toumi, R.: Non-sea-salt-sulphate formation in sea-salt aerosol, *J. Geophys. Res.*, 103, 31095–31102, 1998.
- Council, T., Duckenfield, K., Landa, E., and Callender, E.: Tire-wear particles as a source of zinc to the environment, *Environ. Sci. Technol.*, 38, 4206–4214, 2004.
- David, R. L.: *Handbook of Chemistry and Physics*, 75th Edition, CRC Press, Inc., USA, 1994.
- 25 Draxler, R. R. and Rolph, G. D.: HYSPLIT (HYbrid Single-Particle Lagrangian Integrated Trajectory) Model access via NOAA ARL READY Website. <http://www.arl.noaa.gov/ready/hysplit4.html>, NOAA Air Resources Laboratory, Silver Spring, MD, USA, 2003.
- Decesari, S., Facchini, M. C., Fuzzi, S., and Tagliavini, E.: Characterization of water soluble organic compounds in atmospheric aerosol: A new approach, *J. Geophys. Res.*, 105, 1481–1489, 2000.
- 30

27117

- Espinosa, A. J. F., Rodríguez, M. T., de la Rosa, F. J. B., and Sánchez, J. C. J.: Size distribution of metals in urban aerosols in Seville (Spain), *Atmos. Environ.*, 35, 2595–2601, 2001.
- Grahan, K. K., Hegg, D., Covert, S. D., and Jonsson, H.: An exploration of aqueous oxalic acid production in the coastal marine atmosphere, *Atmos. Environ.*, 38, 3757–3764, 2004.
- 5 Hallquist, M., Wenger, J. C., Baltensperger, U., Rudich, Y., Simpson, D., Claeys, M., Dommen, J., Donahue, N. M., George, C., Goldstein, A. H., Hamilton, J. F., Herrmann, H., Hoffmann, T., Iinuma, Y., Jang, M., Jenkin, M. E., Jimenez, J. L., Kiendler-Scharr, A., Maenhaut, W., McFiggans, G., Mentel, Th. F., Monod, A., Prvt, A. S. H., Seinfeld, J. H., Surratt, J. D., Szmigielski, R., and Wildt, J.: The formation, properties and impact of secondary organic aerosol: current and emerging issues, *Atmos. Chem. Phys.*, 9, 5155–5236, doi:10.5194/acp-9-5155-2009, 2009.
- 10 Hao, Y., Guo, Z., Yang, Z., Fang, M., and Feng, J.: Seasonal variations and sources of various elements in the atmospheric aerosols in Qingdao, China, *Atmos. Res.*, 85, 27–37, 2007.
- Higashi, M., and Takahashi, Y.: Detection of S(IV) species in aerosol particles using XANES spectroscopy, *Environ. Sci. Technol.*, 43, 7357–7363, 2009.
- 15 IPCC Climate Change 2007: Synthesis Report, the Intergovernmental Panel on Climate Change, Cambridge University Press, UK, 2007.
- Kalberer, M., Yu, J., Cocker, D. R., Flagan, R. C., and Seinfeld, J. H.: Aerosol formation in the cyclohexene-ozone system, *Environ. Sci. Technol.*, 34, 4894–4901, 2000.
- 20 Kanai, Y., Ohta, A., Kamioka, H., Terashima, S., Imai, N., Matsuhisa, Y., Kanai, M., Shimizu, H., Takahashi, Y., Kai, K., Xu, B., Hayashi, M., and Zhang, R.: Variation of concentrations and physicochemical properties of aeolian dust obtained in east China and Japan from 2001 to 2002, *Bull. Geol. Surv. Jpn.*, 54, 251–267, 2003.
- Kanakidou, M., Seinfeld, J. H., Pandis, S. N., Barnes, I., Dentener, F. J., Facchini, M. C., Van Dingenen, R., Ervens, B., Nenes, A., Nielsen, C. J., Swietlicki, E., Putaud, J. P., Balkanski, Y., Fuzzi, S., Horth, J., Moortgat, G. K., Winterhalter, R., Myhre, C. E. L., Tsigaridis, K., Vignati, E., Stephanou, E. G., and Wilson, J.: Organic aerosol and global climate modelling: A review, *Atmos. Chem. Phys.*, 5, 1053–1123, 2005, <http://www.atmos-chem-phys.net/5/1053/2005/>.
- 25 Kauppinen, E. I. and Pakkanen, A. T.: Coal combustion aerosols: A field study, *Environ. Sci. Technol.*, 24, 1811–1818, 1990.
- Kawamura, K. and Ikushima, K.: Seasonal changes in the distribution of dicarboxylic acids in the urban atmosphere, *Environ. Sci. Technol.*, 27, 2227–2235, 1993.
- 30

27118

- Kawamura, K. and Sakaguchi, F.: Molecular distributions of water soluble dicarboxylic acids in marine aerosols over the Pacific Ocean including tropics, *J. Geophys. Res.*, 104, 3501–3509, 1999.
- Kawamura, K., Imai, Y., and Barrie, L.: Photochemical production and loss of organic acids in high Arctic aerosols during long-range transport and polar sunrise ozone depletion events, *Atmos. Environ.*, 39, 599–614, 2005.
- Kelly, J. T., Chuang, C. C., and Wexler, A. S.: Influence of dust composition on cloud droplet formation, *Atmos. Environ.*, 41, 2904–2916, 2007.
- Krueger, B. J., Grassian, V. H., Laskin, A., and Cowin, J. P.: The transformation of solid atmospheric particles into liquid droplets through heterogeneous chemistry: Laboratory insights into the processing of calcium containing mineral dust aerosol in the troposphere, *Geophys. Res. Lett.*, 30(3), 1148, doi:10.1029/2002GL016563, 2003.
- Li, W. J. and Shao, L. Y.: Observation of nitrate coatings on atmospheric mineral dust particles, *Atmos. Chem. Phys.*, 9, 1863–1871, doi:10.5194/acp-9-1863-2009, 2009.
- Lim, H. J., Carlton, A. G., and Turpin, B. J.: Isoprene forms secondary organic aerosol through cloud processing: Model simulations, *Environ. Sci. Technol.*, 39, 4441–4446, 2005.
- Lohmann, U. and Leck, C.: Importance of submicron surface-active organic aerosols for pristine Arctic clouds, *Tellus*, 57B, 261–268, 2005.
- Löflunda, M., Kasper-Giebl, A., Schuster, B., Giebl, H., Hitenberger, R., and Puxbaum, H.: Formic, acetic, oxalic, malonic and succinic acid concentrations and their contribution to organic carbon in cloud water, *Atmos. Environ.*, 36, 1553–1558, 2002.
- Manceau, A., Marcus, M. A., and Tamura, N.: Quantitative speciation of heavy metals in soils and sediments by synchrotron X-ray techniques, *Rev. Mineral. Geochem.*, 49, 341–428, 2002.
- Manoli, E., Voutsas, D., and Samara, C.: Chemical characterization and source identification/apportionment of fine and coarse air particles in Thessaloniki, Greece, *Atmos. Environ.*, 36, 949–961, 2002.
- Maria, S. F., Russell, L. M., Gilles, M. K., and Myneni, S. C. B.: Organic aerosol growth mechanisms and their climate-forcing implications, *Science*, 306, 1921–1924, 2004.
- Martell, A. E. and Smith, R. M.: *Critical Stability Constants. Volume 3, Other Organic Ligands*, Plenum, New York, USA, 1977.
- Mikami, M., Shi, G. Y., and Uno, I.: Aeolian dust experiment on climate impact: An overview of Japan-China joint project ADEC, *Global Planet. Change*, 52, 142–172, 2006.

27119

- Mochida, M., Umemoto, N., Kawamura, K., and Uematsu, M.: Bimodal size distribution of C-2-C-4 dicarboxylic acids in the marine aerosols, *Geophys. Res. Lett.*, 30(13), 1672, doi:10.1029/2003GL017451, 2003.
- Novakov, T. and Penner, J. E.: Large contribution of organic aerosols to cloud-condensation-nuclei concentrations, *Nature*, 365, 823–826, 1993.
- Oum, K. W., Lakin, M. J., DeHaan, D. O., Brauers, T., and Finlayson-Pitts, B. J.: Formation of molecular chlorine from the photolysis of ozone and aqueous sea-salt particles, *Science*, 279, 74–77, 1998.
- Peng, C., Chan, M. N., and Chan, C. K.: The hygroscopic properties of dicarboxylic and multifunctional acids: Measurements and UNIFAC predictions, *Environ. Sci. Technol.*, 35, 4495–4501, 2001.
- Rauch, J. N. and Pacyna, J. M.: Earth's global Ag, Al, Cr, Cu, Fe, Ni, Pb, and Zn cycles, *Global Biogeochem. Cy.*, 23, GB2001, doi:10.1029/2008GB003376, 2009.
- Ravel, B. and Newville, M.: ATHENA, ARTEMIS, HEPHAESTUS: Data analysis for X-ray absorption spectroscopy using IFEFFIT, *J. Synchrotron Rad.*, 12, 537–541, 2005.
- Satsumabayashi, H., Kurita, H., Yokouchi, Y., and Ueda, H.: Mono and dicarboxylic acids under long-range transport of air pollution in Japan, *Tellus* 41B, 219–229, 1989.
- Satsumabayashi, H., Kurita, H., Yokouchi, Y., and Ueda, H.: Photochemical formation of particulate dicarboxylic acids under long-range transport in Japan, *Atmos. Environ.*, 24A, 1443–1450, 1990.
- Saxena, P. and Hildemann, L. M.: Water soluble organics in atmospheric particles: A critical review of the literature and application of thermodynamics to identify candidate compounds, *J. Atmos. Chem.*, 24, 57–109, 1996.
- Seinfeld, J. H. and Pandis, S. N.: *Atmospheric Chemistry and Physics: From Air Pollution to Climate Change*, Second Edition, John Wiley and Sons, NY, USA, 2006.
- Sempéré, R., and Kawamura, K.: Low molecular weight dicarboxylic acids and related polar compounds in the remote marine rain samples collected from Western Pacific, *Atmos. Environ.*, 30, 1609–1619, 1996.
- Sullivan, R. C. and Prather, K. A.: Investigations of the diurnal cycle and mixing state of oxalic acid in individual particles in Asian aerosol outflow, *Environ. Sci. Technol.*, 41, 8062–8069, 2007.
- Sullivan, R. C., Moore, M. J. K., Petters, M. D., Kreidenweis, S. M., Roberts, G. C., and Prather, K. A.: Effect of chemical mixing state on the hygroscopicity and cloud nucleation properties

27120

- of calcium mineral dust particles, *Atmos. Chem. Phys.*, 9, 3303–3316, doi:10.5194/acp-9-3303-2009, 2009.
- Takahashi, Y., Kanai, Y., Kamioka, H., Ohta, A., Maruyama, H., Song, Z., and Shimizu, H.: Speciation of sulfate in size-fractionated aerosol particles using sulfur K-edge X-ray absorption near-edge structure, *Environ. Sci. Technol.*, 40, 5052–5057, 2006.
- 5 Takahashi, Y., Miyoshi, T., Higashi, M., Kamioka, H., and Kanai, Y.: Neutralization of calcite in mineral aerosols by acidic sulfur species collected in China and Japan studied by Ca K-edge X-ray Absorption Near-Edge Structure, *Environ. Sci. Technol.*, 43, 6535–6540, 2009.
- Thornton, J. A., Kercher, J. P., Riedel, T. P., Wagner, N. L., Cozic, J., Holloway, J. S., Dube, W. P., Wolfe, G. M., Quinn, P. K., Middlebrook, A. M., Alexander, B., and Brown, S. S.: A large atomic chlorine source inferred from mid-continental reactive nitrogen chemistry, *Nature*, 464, 271–274, 2010.
- 10 Tsigaridis, K. and Kanakidou, M.: Secondary organic aerosol importance in the future atmosphere, *Atmos. Environ.*, 41, 4682–4692, 2007.
- 15 Turpin, B. J., Saxena, P., and Andrews, E.: Measuring and simulating particulate organics in the atmosphere: Problems and prospects, *Atmos. Environ.*, 34, 2983–3013, 2000.
- Var, F., Narita, Y., and Tanaka, S.: The concentration trend and seasonal variation of metals in the atmosphere in 16 Japanese cities shown by the results of National Air Surveillance Network (NASN) from 1974 to 1996, *Atmos. Environ.*, 34, 2755–2770, 2000.
- 20 Warneck, P.: In-cloud chemistry opens pathway to the formation of oxalic acid in the marine atmosphere, *Atmos. Environ.*, 37, 2423–2427, 2003.
- Yao, X., Fang, M., and Chan, C. K.: Size distributions and formation of dicarboxylic acids in atmospheric particles, *Atmos. Environ.*, 36, 2099–2107, 2002.
- Yao, X., Fang, M., and Chan, C. K.: The size dependence of chloride depletion in fine and coarse sea-salt particles, *Atmos. Environ.*, 37, 743–751, 2003.
- 25 Zappoli, S., Andracchio, A., Fuzzi, S., Facchini, M. C. A., Gelencsér, A., Kiss, G., Krivácsy, Z., Molnár, A., Mészáros, E., Hansson, H. C., Rosman, K., and Zebühr, Y.: Inorganic, organic and macromolecular components of fine aerosol in different areas of Europe in relation to their water solubility, *Atmos. Environ.*, 33, 2733–2743, 1999.
- 30 Zhuang, H., Chan, C. K., Fang, M., and Wexler, A. S.: Formation of nitrate and non-sea-salt sulfate on coarse particles, *Atmos. Environ.*, 33, 4223–4233, 1999.

27121

**Table 1.** Stability constant (log K) of oxalate with some metal ions at 25 °C (Martell and Smith, 1977) and the solubility of the complexes in water (David, 1994).

	log K ( $T = 25^{\circ}\text{C}$ )		Solubility mg/100 g
	$I = 0.10\text{ M}$	$I = 0\text{ M}$	
$\text{K}^+$	n.d.	−0.80	33 000*
$\text{Na}^+$	n.d.	n.d.	6300
$\text{Mg}^{2+}$	2.76	3.43	70
$\text{Ca}^{2+}$	n.d.	3.00	0.67
$\text{Cu}^{2+}$	4.84	6.23	2.53
$\text{Zn}^{2+}$	3.88	4.87	0.79
$\text{Pb}^{2+}$	4.00	4.91	0.16

n.d.: no data; \*solubility in hot water; I: ionic strength.

27122

**Table 2.** Fraction of various Ca species at Tsukuba in winter and summer determined by XANES fitting (mol%).

Season	Particle diameter ( $\mu\text{m}$ )	Calcite	Gypsum	Ca oxalate	Ca nitrate	Anhydrite
Winter	>11	31% $\pm$ 2%	38% $\pm$ 4%			31% $\pm$ 4%
	11–7.0	28% $\pm$ 1%	40% $\pm$ 3%			32% $\pm$ 3%
	7.0–4.7	19% $\pm$ 1%	47% $\pm$ 3%			34% $\pm$ 3%
	4.7–3.3	23% $\pm$ 1%	61% $\pm$ 3%			16% $\pm$ 3%
	3.3–2.1		85% $\pm$ 0%			15% $\pm$ 0%
	2.1–1.1		56% $\pm$ 4%	30% $\pm$ 3%	14% $\pm$ 2%	
	1.1–0.65		58% $\pm$ 3%	20% $\pm$ 4%	22% $\pm$ 2%	
	0.65–0.43		37% $\pm$ 3%	63% $\pm$ 3%		
Summer	>11	18% $\pm$ 1%	23% $\pm$ 3%			59% $\pm$ 3%
	11–7.0		50% $\pm$ 3%			50% $\pm$ 3%
	7.0–4.7		71% $\pm$ 3%			29% $\pm$ 3%
	4.7–3.3		71% $\pm$ 3%			29% $\pm$ 3%
	3.3–2.1		67% $\pm$ 4%			33% $\pm$ 4%
	2.1–1.1		63% $\pm$ 3%	11% $\pm$ 2%	26% $\pm$ 2%	
	1.1–0.65		54% $\pm$ 1%	40% $\pm$ 2%	6% $\pm$ 3%	

27123

**Table 3.** Fraction of various Zn species at Tsukuba in winter and summer determined by XANES fitting (mol%).

Season	Particle diameter ( $\mu\text{m}$ )	Zn oxalate	Zn sulfate	Zn chloride	Zn carbonate	Zn sulfide
Winter	> 11			56% $\pm$ 2%	44% $\pm$ 2%	
	11–7.0			59% $\pm$ 4%	41% $\pm$ 4%	
	7.0–4.7			44% $\pm$ 3%	22% $\pm$ 2%	34% $\pm$ 3%
	4.7–3.3			58% $\pm$ 2%	12% $\pm$ 1%	30% $\pm$ 3%
	3.3–2.1		39% $\pm$ 2%	61% $\pm$ 2%		
	2.1–1.1	30% $\pm$ 2%	70% $\pm$ 2%			
	1.1–0.65	63% $\pm$ 4%	37% $\pm$ 4%			
	0.65–0.43	81% $\pm$ 3%	19% $\pm$ 3%			
	< 0.43	83% $\pm$ 6%	17% $\pm$ 6%			
	Summer	> 11			69% $\pm$ 2%	
11–7.0				72% $\pm$ 2%		28% $\pm$ 2%
7.0–4.7				53% $\pm$ 3%		47% $\pm$ 3%
4.7–3.3				94% $\pm$ 1%		6% $\pm$ 1%
3.3–2.1		20% $\pm$ 2%	9% $\pm$ 2%	71% $\pm$ 1%		
2.1–1.1		46% $\pm$ 2%	54% $\pm$ 2%			
1.1–0.65		58% $\pm$ 4%	42% $\pm$ 4%			
0.65–0.43		63% $\pm$ 3%	37% $\pm$ 3%			
< 0.43		98% $\pm$ 6%	2% $\pm$ 6%			

27124



**Table 4.** Fraction of various Zn species at Tsukuba in the winter and summer determined by EXAFS fitting (mol%).

Season	Particle diameter ( $\mu\text{m}$ )	Zn oxalate	Zn sulfate	Zn chloride
Winter	3.3–2.1	2% $\pm$ 1%	33% $\pm$ 3%	65% $\pm$ 2%
	2.1–1.1	28% $\pm$ 2%	72% $\pm$ 2%	
	1.1–0.65	59% $\pm$ 4%	41% $\pm$ 4%	
	0.65–0.43	79% $\pm$ 4%	21% $\pm$ 4%	
Summer	3.3–2.1	26% $\pm$ 2%	41% $\pm$ 17%	33% $\pm$ 15%
	2.1–1.1	38% $\pm$ 8%	62% $\pm$ 8%	
	0.65–0.43	51% $\pm$ 12%	49% $\pm$ 12%	

27125

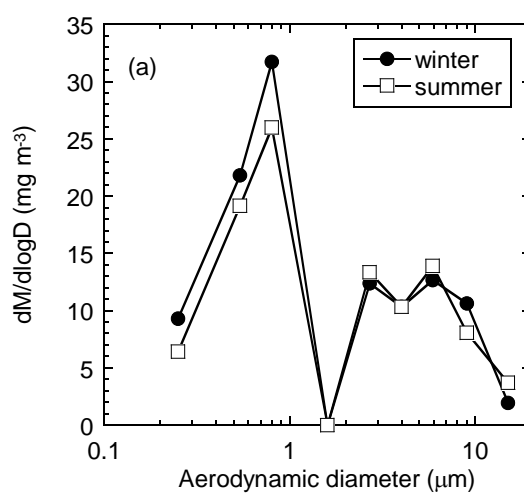


**Fig. 1.** The size distribution of the aerosol mass during winter (21 January to 12 February 2002) and summer (28 July to 13 August 2002) at Tsukuba, Japan.

27126

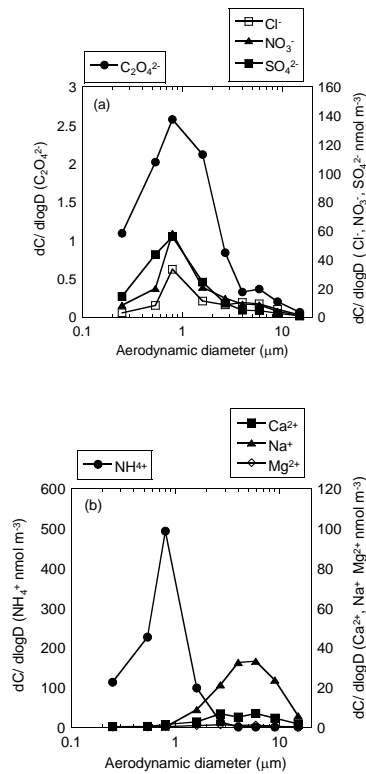


**Fig. 2.** The size distribution of WSCs in aerosols in winter at Tsukuba: **(a)** anions and **(b)** cations.

27127

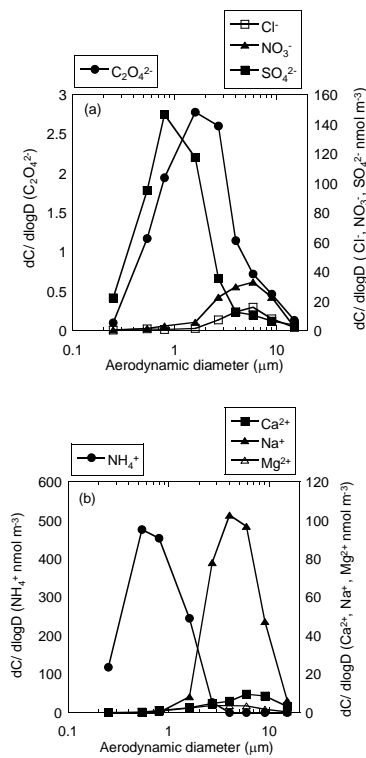


**Fig. 3.** The size distribution of WSCs in aerosols in summer at Tsukuba: **(a)** anions and **(b)** cations.

27128

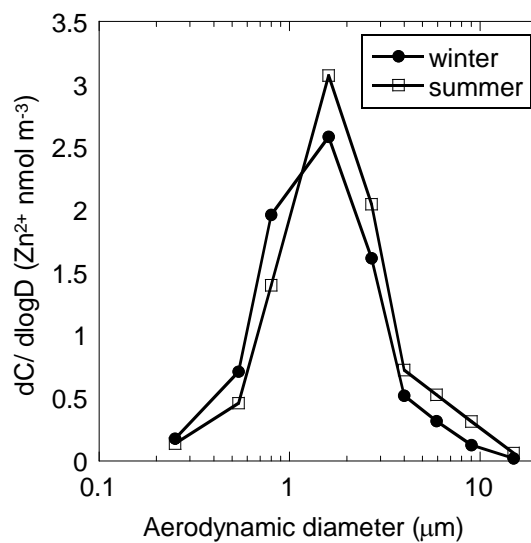


**Fig. 4.** The size distribution of Zn in aerosols during winter and summer at Tsukuba.

27129

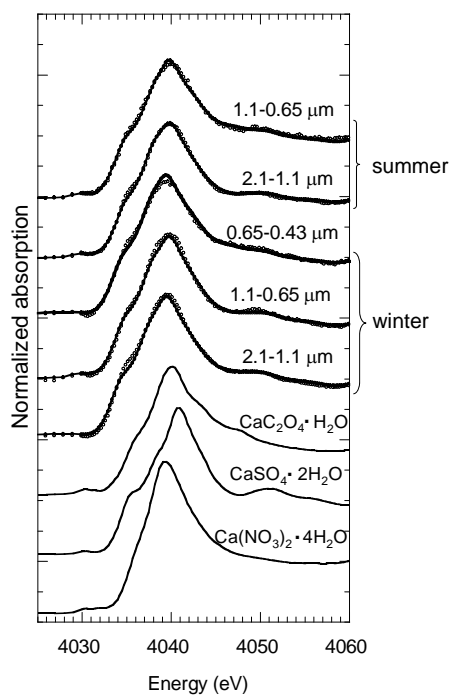


**Fig. 5.** Calcium K-edge XANES spectra (open circles = samples, lines = fitting) of finer particles during winter and summer at Tsukuba with those of the standard materials used for fitting.

27130

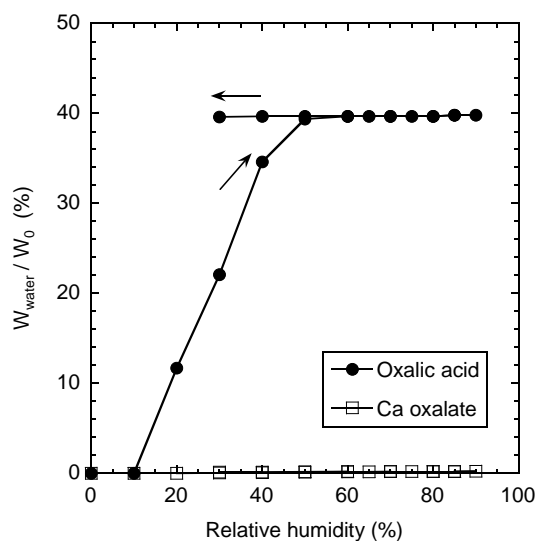


**Fig. 6.** The experimental hygroscopic properties of oxalic acid and a Ca oxalate complex.

27131

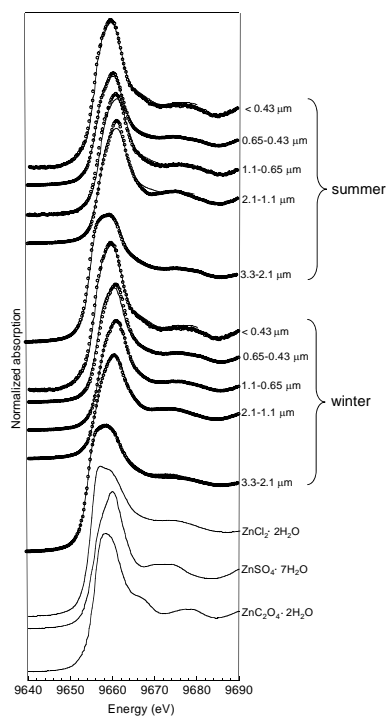


**Fig. 7.** Zinc K-edge XANES spectra (open circles = samples, lines = fitting) of finer particles during winter and summer at Tsukuba with those of the standard materials used for fitting.

27132

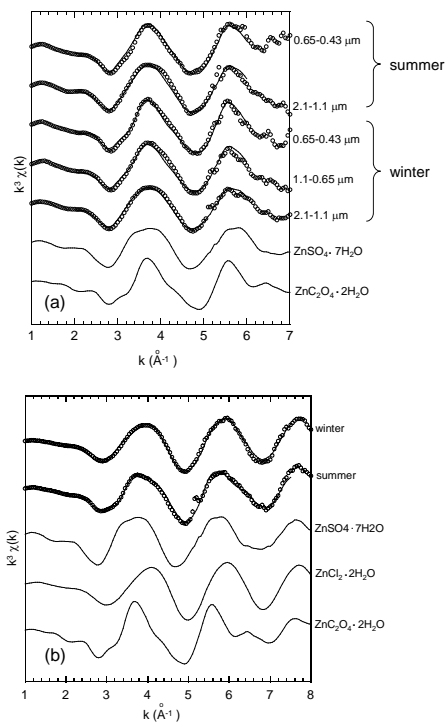


**Fig. 8.** Zinc K-edge EXAFS spectra (open circles = sample, lines = fitting) of finer particles during winter and summer at Tsukuba with standard materials used for fitting: **(a)** 2.1–1.1, 1.1–0.65 μm and 0.65–0.43 μm in winter, and 2.1–1.1 and 0.65–0.43 μm in summer, and **(b)** 2.1–3.3 μm in winter and summer.

27133

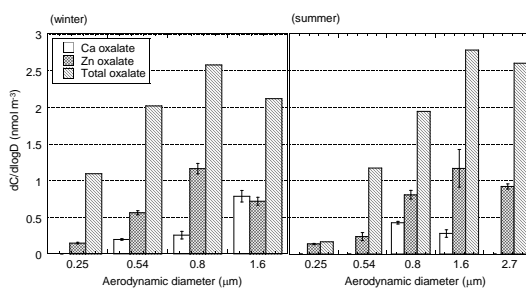


**Fig. 9.** Atmospheric concentrations of Ca oxalate, Zn oxalate, and total oxalate during winter and summer.

27134